

Structure and Thermophysical Properties of Fullerene C₆₀ Aqueous Solutions

Yu. I. Prylutskyy,^{1,2} S. S. Durov,³ L. A. Bulavin,³ I. I. Adamenko,³
K. O. Moroz,³ I. I. Geru,⁴ I. N. Dihor,⁴ P. Scharff,⁵
P. C. Eklund,⁶ and L. Grigorian⁶

Received June 26, 2000

The structure and thermophysical properties of fullerene C₆₀ aqueous solutions were investigated both experimentally and theoretically. The aggregation kinetics results indicated that the structure of fullerene C₆₀ aggregates in water could be described as a fractal system. The IR and electronic absorption spectra obtained confirm the presence of the crystalline phase in aqueous solution. The numerical values of thermodynamic coefficients α_P , β_T , β_S , c_P , and c_V , and sound velocity were determined from the measured (P - V - T) data. The vibrational spectrum of the crystalline structure (T_h symmetry group) formed from the hydrated single fullerene C₆₀ molecules in aqueous solutions was calculated using the molecular dynamics approach.

KEY WORDS: fullerene C₆₀ aqueous solution; IR and electronic absorption spectra; molecular dynamics approach; thermophysical properties.

1. INTRODUCTION

Fullerenes are currently being widely investigated and have potential for various technical applications [1]. In particular, for biomedical testing, water-soluble forms of fullerenes are of great interest. Recently, Andrievsky

¹ Department of Biophysics, Kyiv National Shevchenko University, Volodymyrska Str. 64, 01033 Kyiv, Ukraine.

² To whom correspondence should be addressed. E-mail: prylut@biocc.univ.kiev.ua

³ Department of Physics, Kyiv National Shevchenko University, Volodymyrska Str. 64, 01033 Kyiv, Ukraine.

⁴ Department of Physics, State University of Moldova, Chisinau MD 009, Moldova.

⁵ Institute of Physics, TU Ilmenau, PF 100565, D-98684 Ilmenau, Germany.

⁶ Department of Physics, Penn State University, University Park, Pennsylvania 16802-6300, U.S.A.

and co-workers [2–4] proposed a method for obtaining aqueous solutions of fullerene C_{60} without any stabilizers and chemical modification. These dark brownish–orange fullerene C_{60} water solutions are stable over periods of 12 to 18 months and even longer on storage under normal conditions of 4 to 40°C. The maximum concentration of fullerene C_{60} reached in a water solution is approximately $2.3 \text{ g} \cdot \text{L}^{-1}$ (for comparison, the solubilities of C_{60} are 1.7 and $2.9 \text{ g} \cdot \text{L}^{-1}$ in benzene and toluene, respectively). Fullerene C_{60} aqueous solutions are shown to be ultramicroheterogeneous and polydisperse systems containing spherical C_{60} aggregates (both single fullerene C_{60} molecules and their fractal clusters, with diameters from 3.4 to 36 nm) in a hydrated state (i.e., the fullerene aggregates are covered by a strong hydrated shell). Moreover, the crystalline phase, observed experimentally in fullerene C_{60} aqueous solutions, consists of spherical C_{60} aggregates 1 to 4 nm in size. Hence, more detailed theoretical and experimental studies of the structure, vibrational, and thermodynamic properties of fullerene C_{60} aqueous solutions are important.

2. THEORY AND EXPERIMENTAL

2.1. Structure of Fullerene C_{60} Clusters in Aqueous Solution

Let us assume that the formation of clathrate-like networks of water molecules around fullerene C_{60} aggregates, stabilized due to the low conformational mobility of fullerenes and geometrical matching between the structures, by hydrogen bonding of water molecules in the clathrate and covalent bonds of the fullerene carbon atoms, takes place [2–4].

The free energy of the system “fullerene C_{60} cluster + aqueous solution” at temperature T includes the following contributions.

$$E = U_1 + U_2 + U_3 - T \Delta S \quad (1)$$

(1) Within the cluster. A Lennard–Jones (12–6) atom–atom potential and an electrostatic potential of charges are located on single and double bonds of the C_{60} molecule:

$$U_1 = \sum_{\mu, \mu'} \left\{ 4\epsilon \sum_{i,j} \left[\left(\frac{\sigma}{|\mathbf{r}_{\mu i} - \mathbf{r}_{\mu' j}|} \right)^{12} - \left(\frac{\sigma}{|\mathbf{r}_{\mu i} - \mathbf{r}_{\mu' j}|} \right)^6 \right] + \sum_{m,n} \frac{q_m q_n}{|\mathbf{r}_{\mu m} - \mathbf{r}_{\mu' n}|} \right\} \quad (2)$$

Here, $\mathbf{r}_{\mu i}$ and $\mathbf{r}_{\mu m}$ are the coordinates of the i th carbon atom and m th bond center in the molecule μ , respectively; and q_m is the effective charge of the m th bond and equals q in the case of a single bond and $-2q$ for a double bond. The values of the parameters ϵ , σ , and q were taken from our previous paper on the simulation of the solid C_{60} structure [5].

(2) Within the water medium. A dipole–dipole interaction of water molecules (the first coordination sphere) occurs:

$$U_2 = \sum_{v, v'} \left\{ \frac{\mathbf{d}_v \cdot \mathbf{d}_{v'}}{r_{vv'}^3} - \frac{3(\mathbf{d}_v \cdot \mathbf{r}_{vv'})(\mathbf{d}_{v'} \cdot \mathbf{r}_{vv'})}{r_{vv'}^5} \right\} \quad (3)$$

Here, $d_v = 1.6$ D is the dipole moment of a single water molecule v .

(3) Outside the cluster. A polarization interaction of each C₆₀ molecule in the cluster with the water medium occurs:

$$U_3 = -\alpha \sum_{v, v'} \frac{d_v^2(\theta_{v, v'})}{r_{vv'}^6} \quad (4)$$

Here, $\alpha = 8.48 \times 10^{-2} \text{ nm}^3$ is the polarizability of a single fullerene C₆₀ molecule [6] and $\theta_{vv'}$ is the angle between the dipole moment of water molecule that of water molecule v and v' .

(4) Entropy. The isothermal change in the entropy ΔS for the system “fullerene C₆₀ cluster + aqueous solution” has been calculated by the formula

$$\Delta S = - \int \left(\frac{\partial V}{\partial T} \right)_P dP \quad (5)$$

The results obtained are shown in Fig. 1.

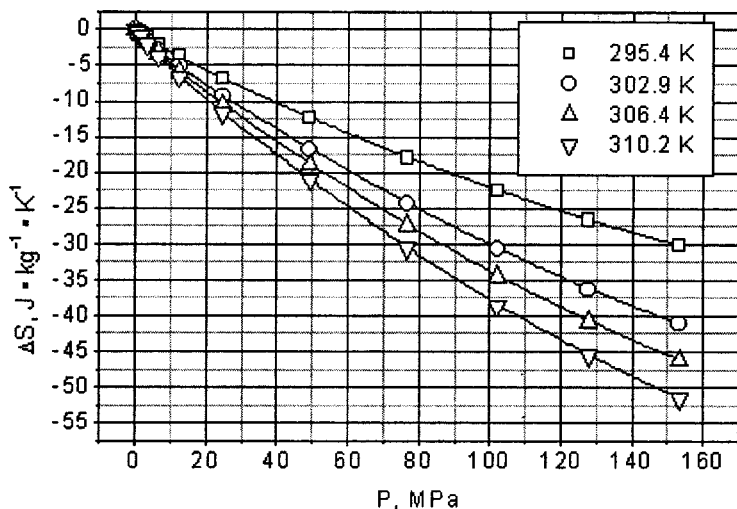


Fig. 1. Calculated isothermal change in entropy for fullerene C₆₀ aqueous solutions.

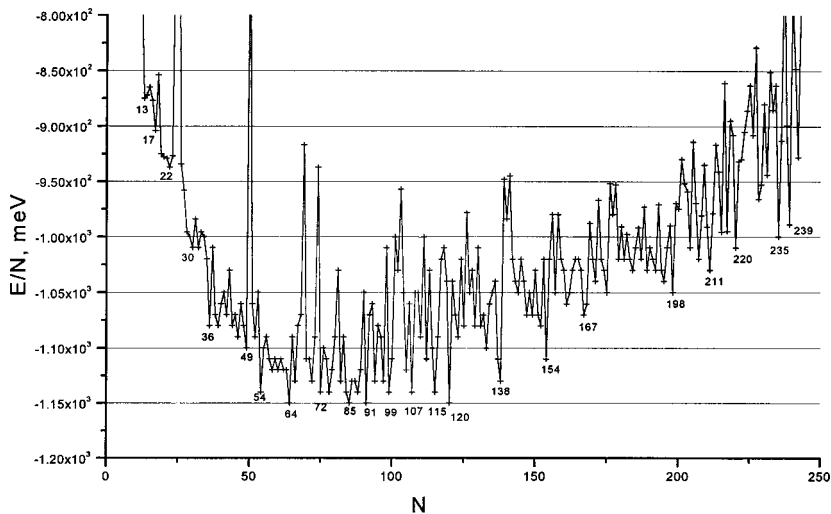


Fig. 2. Calculated energy (normalized to one molecule) of possible clusters in aqueous solutions versus the number of single molecules C_{60} entering them.

The minimization of the free energy [Eq. (1)] was performed using the dense-packing principle. The calculated energy (normalized to one molecule) of possible hydrated $(C_{60})_N$ clusters plotted against the number of single molecules C_{60} entering them is shown in Fig. 2. As shown, the smallest stable fullerene C_{60} cluster (I_h symmetry group) consists of 13 C_{60} molecules. Its diameter is 3.36 nm (accounting for a molecular diameter of the water molecule of ~ 0.28 nm [7, 8]). This result is in excellent agreement with the scanning tunneling microscopy data [3, 4], which confirm that the smallest stable spherical clusters in fullerene C_{60} aqueous solutions have a mean size of 3.4 nm. Other clusters presented in Fig. 2 are stable (numbered clusters) or partly stable (unnumbered clusters) in aqueous solutions.

Let us remember that, without stresses of valency angles, the diameter of the shell formed from the water molecules around the dissolved aggregate can be increased to 2 nm [7] and, within the admissible stresses of hydrogen bonds, can be increased to even 6 nm [8]. The results obtained for stable fullerene $(C_{60})_N$ clusters with a number of molecules $13 \leq N \leq 120$ do not contradict this fact. On the other hand, it is known [9] that water has a cluster structure and the diameter of these clusters is 10 nm. The size of $(C_{60})_N$ clusters with a number of molecules $13 \leq N \leq 239$ does not exceed this value. Hence, a fullerene C_{60} aqueous solution may combine some properties of a typical colloidal solution with those of a true molecular solution.

2.2. Aggregation of Fullerene C₆₀ in Aqueous Solution

According to the fractal concept [10], two limiting regimes of irreversible colloids, namely, reaction-limited cluster aggregation (RLCA; a slow aggregation process) and diffusion-limited cluster aggregation (DLCA; a fast aggregation process), have been used to characterize the structure and kinetics of colloidal fractal aggregates. The fractal dimension d_f is approximately 2.1 for RLCA, which exhibits exponential kinetics, $M \sim e^{Bt}$, where M and B are the average mass of the cluster and a constant, respectively. For DLCA, $d_f \approx 1.8$ and M increases linearly with time.

The increase in the average molar mass M as a function of aggregation time is shown in Fig. 3. As shown, the linear dependence obtained (the continuous curve in Fig. 3) reflects the fast aggregation process directly (i.e., the DLCA case).

According to the DLCA theory, the relationship among the number of particles in a cluster (N), its radius (R), and its fractal dimensionality (d_f) has the form [10]

$$N = \left(\frac{R}{r}\right)^{d_f} \quad (6)$$

where r is the radius of a particle forming the cluster. In accordance with Eq. (6) and with the values $N = 13$, $R = 1.4$ nm [the radius of the smallest

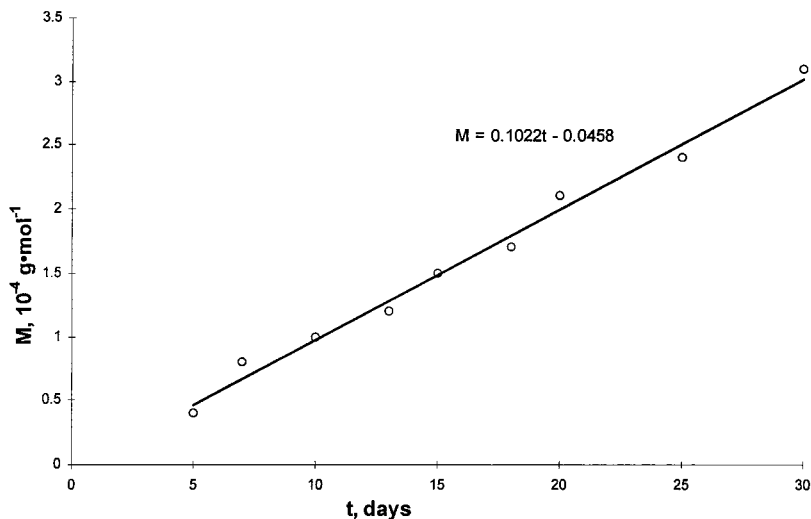


Fig. 3. Plot of weight-averaged molar mass M as a function of aggregation time for a sample with a concentration $1.1 \text{ g} \cdot \text{L}^{-1}$.

stable $(C_{60})_{13}$ cluster without accounting for the molecular diameter of the water molecule], and $r = 0.35$ nm (the radius of a single C_{60} molecule [11]), we found that $d_f \approx 1.85$, which confirms the above experimental result ($d_f \approx 1.8$).

By analyzing the sizes of the observed fullerene C_{60} spherical particles in water, Andrievsky and co-workers [3, 4] revealed that their diameters regularly rise within the range from 3.4 to 36 nm and are 3.4, 7.1, 10.9, 14.5, 18.1, 21.8, 25.4, 28.8, 32.4, and 36.0 nm. Taking the smallest hydrated spherical $(C_{60})_{13}$ cluster, with a diameter of 3.4 nm (3.36 nm according to our theoretical calculations), as the first member, we can see that each following particle is larger than the preceding one by 3.4 to 3.8 nm. Note that the regularity found for the observed spherical particles will be valid only if the cluster of size 3.4 nm is taken as the primary one. Hence, one can assume that the above row of fullerene C_{60} particles should be formed of hydrated $(C_{60})_{13}$ clusters.

2.3. Optical Spectra of Fullerene C_{60} Aggregates in Aqueous Solutions

According to the one-electron model, the C_{60} molecule ground state consists of five occupied orbital states (HOMO) of h_u symmetry, each having double-spin degeneration [12]. The lowest unoccupied molecular orbitals are three t_{1u} symmetric double-spin degenerate states (LUMO). For one-electron electric dipole $h_u \leftrightarrow t_{1u}$ transitions (HOMO \leftrightarrow LUMO) with photons, absorption or emission is forbidden due to the same parity (the respective wave functions are odd) of the orbital states. The first dipole-allowed transition, corresponding to the minimum excitation energy of molecule C_{60} , is $h_u \leftrightarrow t_{1g}$ (HOMO \leftrightarrow "LUMO + 1 state"). Dipole-allowed transitions in order of increasing molecule excitation energy are as follows: $(h_g + g_g) \leftrightarrow t_{1u}$ (HOMO - 1 \leftrightarrow LUMO), $h_u \leftrightarrow h_g$ (HOMO \leftrightarrow LUMO + 3), and $(h_g + g_g) \leftrightarrow t_{2u}$ (HOMO - 1 \leftrightarrow LUMO + 2) [1]. Interactions between C_{60} molecules in solution and in the fullerite do not significantly change the molecular orbital electronic wave functions [13, 14]. Therefore, the structure of the electronic spectrum of free C_{60} molecules and fullerene molecules in the fluid or in the crystalline state must differ slightly. Herewith, the transition from the noninteracting molecule state to condensed ones is accompanied by small shifts of lines in the optical spectrum and their widening. This is confirmed experimentally. Fullerene C_{60} aggregates in water spectral absorption coefficient dependence in the UV-vis range 1.6 to 6.2 eV is shown in Fig. 4. Four intensive lines of absorption, with maxima at 2.92, 3.62, 4.66, and 5.63 eV, are related to the dipole-allowed transitions specified above. The positions of these lines are in good agreement with the data on ellipsometric and optical transparency measurements for

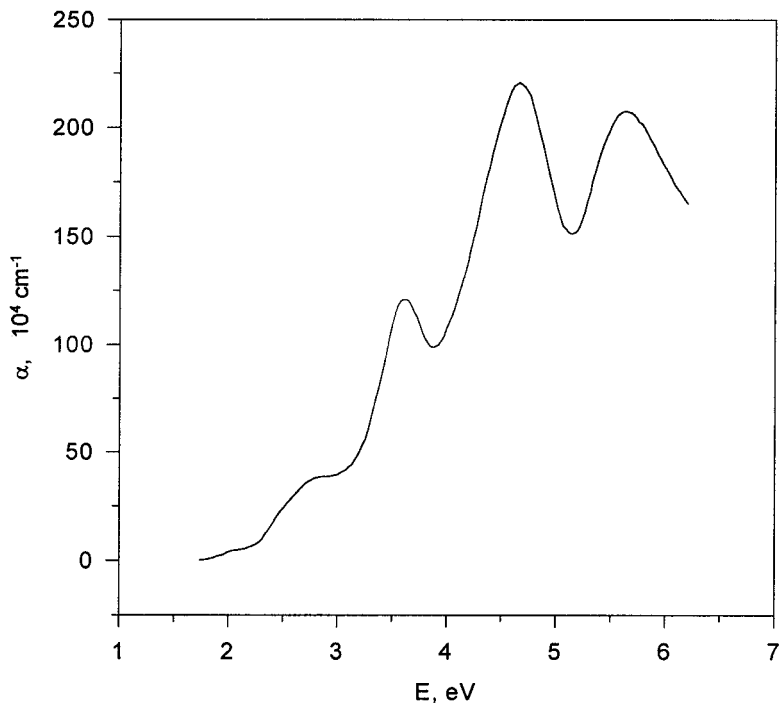


Fig. 4. Dependence of the optical absorption coefficient of fullerene C_{60} aggregates in aqueous solutions as a function of energy in the UV-vis range.

crystalline C_{60} [6, 15–18]. Also, in accordance with the above, the UV-vis absorption spectrum of fullerite nanostructure differs insignificantly from the C_{60} molecule spectrum in *n*-hexane (3.7, 4.6, and 5.8 eV [6]) or in decaline (~ 3 , 3.6, 4.7, and 5.7 eV [19]). The half-widths of lines with maxima at 3.62, 4.66, and 5.63 eV are in the interval 0.25 to 0.66 eV, but the line with a maximum at 2.92 eV has a width of ~ 0.05 eV. A line of low intensity caused by the optical dipolar-forbidden transition $h_u \leftrightarrow t_{1u}$ (Fig. 4) is also observed in the range of the fundamental absorption edge (~ 2 eV). Thus, dipole-forbidden optical transitions, with increasing photon energy, turn into dipole-allowed optical transitions, with simultaneous increases in absorption line intensities. Indeed, in the case of an optical transition, the square of the matrix element of the dipole momentum operator between the initial and the final states is a function of the photon energy.

Though the electronic spectra of fullerene C_{60} molecules in the fluid and crystalline states show insignificant differences, the presence of the fullerite nanostructure in water can be observed experimentally in optical

spectra. For this, it is necessary to prove the existence of indirect optical transitions, which are typical for the crystalline state. The spectral profiles of direct allowed, indirect allowed, and indirect forbidden transitions are obtained from the absorption spectrum in Fig. 4 according to the relation $(E\alpha)_\gamma = f(E)$, where α is the absorption coefficient, E is the energy of photons, and $\gamma = \frac{2}{3}, 2, \frac{1}{2},$ and $\frac{1}{3}$ for direct forbidden, direct allowed, indirect allowed, and indirect forbidden transitions, respectively. This treatment, as is well known, is used in the theory of semiconductors for the determination of optical transition types. The existence of direct allowed optical transitions [$h_u \leftrightarrow t_{1g}, (h_g + g_g) \leftrightarrow t_{1u}, h_u \leftrightarrow h_g, (h_g + g_g) \leftrightarrow t_{2u}$], indirect allowed optical transitions [$h_u \leftrightarrow t_{1g}, (h_g + g_g) \leftrightarrow t_{1u}$], and indirect forbidden optical transitions [$h_u \leftrightarrow t_{1g}, (h_g + g_g) \leftrightarrow t_{1u}$] in fullerene C_{60} aggregates in water is shown in Figs. 5 and 6. The E_g values for direct and indirect dipole-forbidden and dipole-allowed transitions, as well as the phonon energy, of the indirect optical transitions, are given in Table I. The γ index in Table I indicates the $(E\alpha)$ product degree in the $(E\alpha)_\gamma = f(E)$ relation. We note that in Table I the transition types are marked with the same symbols, $h_u \leftrightarrow t_{1g}$ and $(h_g + g_g) \leftrightarrow t_{1u}$, for both direct and indirect transitions, respectively. Truly, the final state of the indirect transition corresponds to wave vector $\mathbf{k} = \mathbf{k}_0 \neq 0$ and it is transformed as the irreducible representation of the wave vector $G_{\mathbf{k}0}$ group. The final-state symmetries for two specified types of indirect transition should be elucidated. We mention also that in the case of the indirect forbidden transition $(h_g + g_g) \leftrightarrow t_{1u}$, the phonon energy $E_{ph} = 1900.0 \text{ cm}^{-1}$ exceeds the limiting energy for "intern" phonons of fullerite C_{60} . It is possible that two phonons with a total energy equal to 1900.0 cm^{-1} participate in this transition.

Thus, the structure and parameters of an electronic spectrum (Figs. 4–6 and Table I) indicate the presence of fullerene C_{60} molecules in the investigated liquid. The indirect optical transitions revealed in this case

Table I. Energy Gaps Determined from Direct and Indirect Optical Transitions Data for Fullerene C_{60} Aggregates in Aqueous Solutions

Type of transition	Direct forbidden,	Direct allowed,	Indirect allowed		Indirect forbidden	
	E_g (eV)	E_g (eV)	E_g (eV)	E_{ph} (cm^{-1})	E_g (eV)	E_{ph} (cm^{-1})
$h_u \leftrightarrow t_{1u}$	1.77	—	—	—	—	—
$h_u \leftrightarrow t_{1g}$	—	2.37	1.89	879.3	1.71	903.5
$(h_g + g_g) \leftrightarrow t_{1u}$	—	3.27	2.56	1097.1	2.14	1900.0
$h_u \leftrightarrow h_g$	—	4.02	—	—	—	—
$(h_g + g_g) \leftrightarrow t_{2u}$	—	4.90	—	—	—	—
γ	2/3	2		1/2		1/3

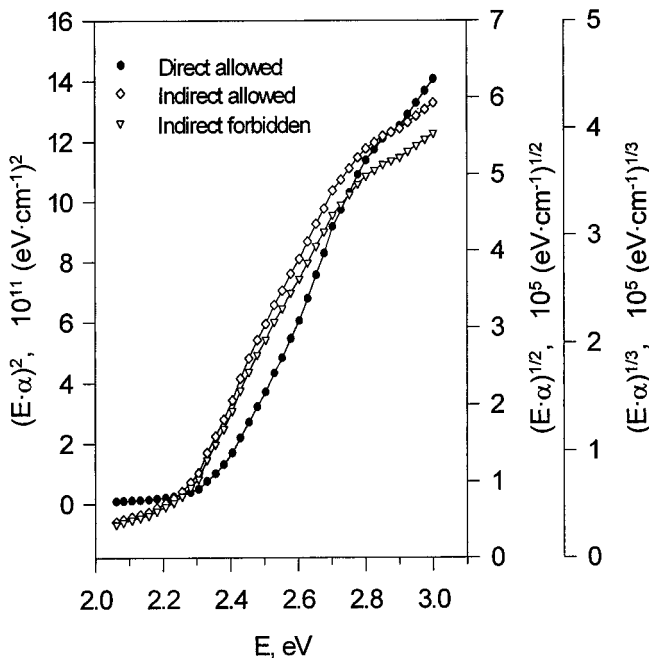


Fig. 5. Direct allowed transitions (●), indirect allowed transitions (◇), and indirect forbidden transitions (▽) in fullerene C₆₀ aggregates in aqueous solutions in the 2.1- to 3.0-eV range.

unequivocally prove the existence of the crystalline state of fullerene molecules as fullerene C₆₀ aggregates in the aqueous solution.

2.4. Vibrational Spectrum of Fullerene C₆₀ Crystal in Aqueous Solutions

Earlier we found [20] that the values of vibrational Raman frequencies of fullerene C₆₀ aqueous solutions increase in comparison with results for individual C₆₀ molecules [21] by a magnitude of 2 to 6%. This increase is associated with a strengthening of the intramolecular bonds on forming the hydrated fullerene C₆₀ aggregates in aqueous solutions described above. In other words, the effect of water amounts to external hydrostatic compression of the C₆₀ molecules in the aggregate, leading to a negligible decrease in its geometrical size and an increase in bond energy.

As is known, C₆₀ molecules rotate freely in a solid at room temperature [22]. In our opinion, the effect of water on the forming crystal structures is connected with the fixation of hydrated C₆₀ molecules' orientation in the unit cell of the lattice (i.e., a transition from a disordered structure

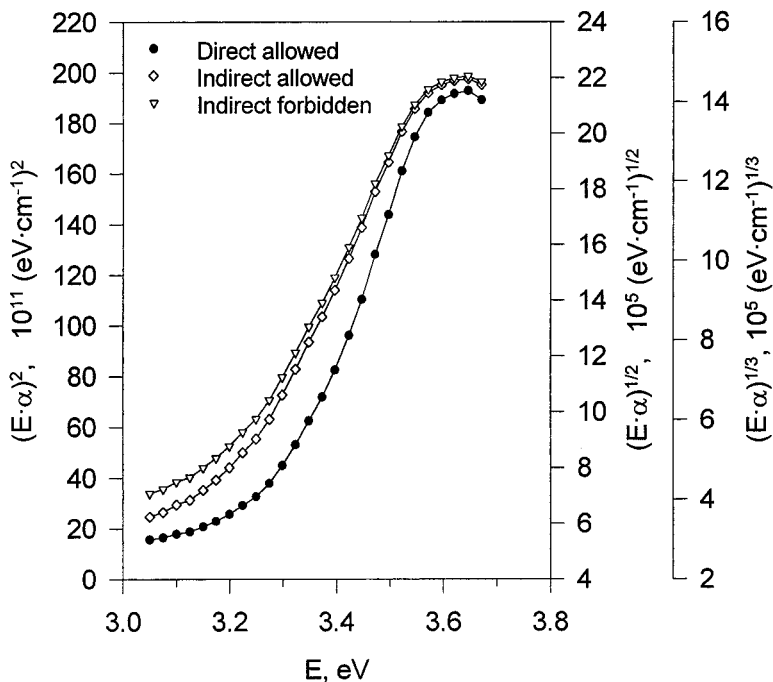


Fig. 6. Direct allowed transitions (●), indirect allowed transitions (◇), and indirect forbidden transitions (▽) in fullerene C_{60} aggregates in aqueous solutions in the 2.9- to 3.7-eV range.

to an orientationally ordered crystalline phase [23] takes place). Thus, we consider the following structure of solid C_{60} in aqueous solutions: the number of hydrated C_{60} molecules in the unit cell is $Z=4$, the space group is T_h , and the lattice constant is $a=1.85$ nm (for comparison, $a=1.40$ nm for solid C_{60} [23]).

The minimization of the free energy of a C_{60} crystal in an aqueous solution,

$$E = U_1 + U_2 + U_3 \quad (7)$$

was performed using the atom-atom potential method described in detail in our previous paper [24]. In particular, it was found that the minimum of the lattice energy for solid C_{60} in an aqueous solution $E_{\min} = -2.5$ eV (for comparison, $E_{\min} = -1.9$ eV for solid C_{60} [24]).

The values of fundamental intermolecular frequencies of C_{60} crystals in aqueous solutions in the center of the Brillouin zone ($\mathbf{k} = 0$) were calculated based on analytical formulas [24]. The results obtained are

Table II. Frequencies (cm⁻¹) of Intermolecular Modes in the Center of the Brillouin Zone

Symmetry	Solid C ₆₀ (theory [24])	Crystal C ₆₀ in aqueous solution	
		Theory	Experiment
A _u	35.0	26.9	
E _u	46.7	35.9	
F _u	42.9	33.0	36.6
F _u	51.0	39.2	41.9
A _g	18.6	14.3	
E _g	18.5	14.2	
F _g	17.1	13.2	
F _g	17.5	13.5	
F _g	22.0	16.9	

represented in Table II. It is seen that the calculated vibrational frequencies for C₆₀ crystals in aqueous solutions are located lower than the calculated fundamental modes for solid C₆₀ [24]. All g modes are Raman active, and only two F_u modes are IR active. The theoretical values are different from the experimental data obtained for the IR modes by up to 11%.

2.5. Thermophysical Properties of Fullerene C₆₀ Aqueous Solution

The (*P-V-T*) data of fullerene C₆₀ aqueous solutions (Fig. 7) were measured by use of the metallic bellows method with a differential inductive sensor of linear shifts in the temperature range of 295 to 310 K and pressure range of 0.1 to 153 MPa. As a result, we found the numerical values for the isobaric coefficient of thermal expansion, $\alpha_P = 4.0 \times 10^{-4} \text{ K}^{-1}$, and for the isothermal compressibility, $\beta_T = 2.20 \times 10^{-4} \text{ MPa}^{-1}$ (for comparison, $\beta_T = 4.70 \times 10^{-4} \text{ MPa}^{-1}$ for water), under ambient conditions using the following formulas [25]:

$$\alpha_P = \frac{1}{V} \left(\frac{dV}{dT} \right)_P \quad (8)$$

$$\beta_T = -\frac{1}{V} \left(\frac{dV}{dP} \right)_T$$

The value of the adiabatic compressibility coefficient β_S was calculated from the following equation [25]:

$$\beta_S = \frac{1}{v_S^2 \rho} \quad (9)$$

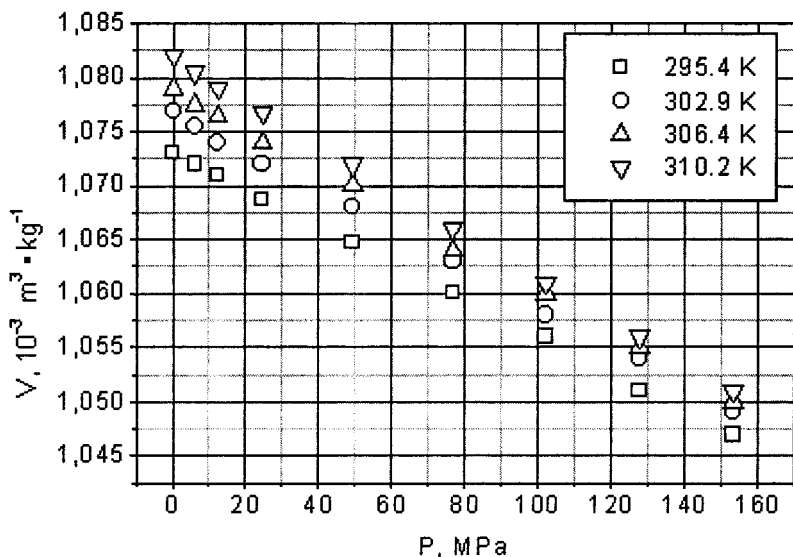


Fig. 7. The (P - V - T) data on fullerene C_{60} aqueous solutions.

where $v_S = 1.77 \text{ km} \cdot \text{s}^{-1}$ (for comparison, $v_S = 1.50 \text{ km} \cdot \text{s}^{-1}$ for water) is the sound speed and $\rho = 1754 \text{ kg} \cdot \text{m}^{-3}$ is the density of the fullerene C_{60} aqueous solution under ambient conditions. Note that on the liquid-vapor equilibrium line the density was measured using the pycnometer method. The sound speed was measured by the direct pulse method of fixed distance. It turned out that $\beta_S = 1.82 \times 10^{-4} \text{ MPa}^{-1}$ under ambient conditions.

The values of the molar heat capacity c_P and c_V were found from the equations [25]

$$c_P = \frac{\alpha_p^2 T}{\rho(\beta_T - \beta_S)} \quad (10)$$

$$c_V = c_P \frac{\beta_S}{\beta_T} \quad (11)$$

It turned out that $c_P = 72.0 \text{ J} \cdot \text{mol}^{-1} \cdot \text{K}^{-1}$ and $c_V = 59.6 \text{ J} \cdot \text{mol}^{-1} \cdot \text{K}^{-1}$ under ambient conditions.

3. CONCLUSION

We have demonstrated that fullerene C_{60} molecules in aqueous solutions can aggregate rapidly at room temperature. The kinetic study showed

that the structure of C₆₀ aggregates can be described as a fractal with a dimension of 1.8 to 1.85. The hydrated spherical cluster (I_h symmetry group) with a diameter of 3.36 nm, containing 13 molecules C₆₀, was shown to be the smallest stable form among all the possible aggregates. By analyzing the sizes of the observed fullerene C₆₀ spherical particles in aqueous solutions [3, 4], we found that these aggregates should be formed of hydrated (C₆₀)₁₃ clusters. The optical absorption spectra of C₆₀ aqueous solutions demonstrate the crystalline character of absorption. The calculated intermolecular spectrum of C₆₀ crystals (T_h symmetry group) in aqueous solutions was found to be in satisfactory agreement with IR spectroscopic data. The thermophysical characteristics (α_P , β_T , β_S , c_P , c_V , and sound speed) of fullerene C₆₀ aqueous solutions were determined.

ACKNOWLEDGMENTS

This work was supported by a CR NATO grant. The authors thank Dr. G. V. Andrievsky for kindly providing the fullerene C₆₀ aqueous solutions.

REFERENCES

1. M. S. Dresselhaus, G. Dresselhaus, and P. C. Eklund, *Science of Fullerenes and Carbon Nanotubes* (Academic Press, New York, 1996).
2. N. O. Mchedlov-Petrosyan, V. K. Klochkov, and G. V. Andrievsky, *J. Chem. Soc. Faraday Trans.* **93**:4343 (1997).
3. G. V. Andrievsky, V. K. Klochkov, E. L. Karyakina, and N. O. Mchedlov-Petrosyan, *Chem. Phys. Lett.* **300**:392 (1999).
4. G. V. Andrievsky, V. K. Klochkov, and L. I. Derevyachenko, 4th Biennial International Workshop in Russia: Fullerenes and Atomic Clusters, Abstracts of Invited Lectures and Contributed Papers, St. Petersburg (1999), p. 169.
5. Yu. I. Prilutski, E. V. Buzaneva, L. A. Bulavin, and P. Scharff, *Carbon* **37**:835 (1999).
6. S. L. Ren, Y. Wang, A. M. Rao, E. McRae, J. M. Holden, T. Hager, K. Wang, W. T. Lee, J. Selegue, and P. C. Eklund, *Appl. Phys. Lett.* **59**:2678 (1991).
7. S. P. Gabuda, *Combined Water. Facts and Hypotheses* (Nauka, Novosibirsk, 1982).
8. S. Wei and A. W. Castlemann, *Int. J. Mass Spectr. Ion Process.* **131**:233 (1994).
9. G. V. Yukhnevich and V. V. Volkov, *Dokl. Akad. Nauk* **353**:465 (1997).
10. B. M. Smirnov, *Physics of Fractal Aggregates* (Nauka, Moscow, 1991).
11. H. W. Kroto, J. R. Heath, S. C. O'Brein, R. F. Curl, and R. E. Smalley, *Nature* **318**:162 (1985).
12. R. C. Haddon, *Acc. Chem. Res.* **25**:127 (1992).
13. S. Saito, S. Sawada, and R. Zanasi, *Chem. Phys. Rev. B.* **45**:6912 (1992).
14. C. H. Xu and G. E. Scuseria, *Phys. Rev. Lett.* **72**:669 (1994).
15. G. Gensterblum, J. J. Pireaux, P. A. Thiry, R. Caudano, J. P. Vigneron, P. Lambin, A. A. Lucas, and W. Kratschmer, *Phys. Rev. Lett.* **67**:2171 (1991).
16. E. Sohmen and J. Fink, *Phys. Rev. B* **47**:14532 (1993).
17. S. Modesti, S. Gerasari, and P. Rudolf, *Phys. Rev. Lett.* **71**:2469 (1993).
18. V. I. Srdanov, C. H. Lee, and N. S. Sariciftci, *Thin Sol. Films* **257**:233 (1995).

19. S. Leach, M. Vervloet, A. Despres, E. Breheret, J. P. Hare, T. J. Dennis, H. W. Kroto, and D. R. M. Walton, *Chem. Phys.* **160**:451 (1992).
20. Yu. I. Prilutski, S. S. Durov, V. N. Yashchuk, T. Yu. Ogul'chansky, V. E. Pogorelov, Yu. A. Astashkin, E. V. Buzaneva, Yu. D. Kirghizov, G. V. Andrievsky, and P. Scharff, *Eur. Phys. J. D* **9**:341 (1999).
21. D. S. Bethune, G. Meijer, W. C. Tang, H. J. Rosen, W. G. Golden, H. Seki, C. A. Brown, and M. S. de Vries, *Chem. Phys. Lett.* **179**:181 (1991).
22. W. Kratschmer, L. D. Lamb, K. Fostiropoulos, and D. R. Huffman, *Nature* **347**:354 (1990).
23. W. I. F. David, R. M. Ibberson, J. C. Matthewman, K. Prassides, T. J. S. Dennis, J. P. Hare, H. W. Kroto, R. Taylor, and D. R. M. Walton, *Nature* **353**:147 (1991).
24. Yu. I. Prilutski and G. G. Shapovalov, *Phys. St. Sol. (b)* **201**:361 (1997).
25. J. O. Hirschfelder, Ch. F. Curtiss, and R. B. Bird, *Molecular Theory of Gases and Liquids* (John Wiley, New York, 1954).